Optical continua generation in a coherently prepared Raman medium

Roman Kolesov

Department of Physics and Institute for Quantum Studies, Texas A&M University, College Station, Texas 77843-4242
and Institute of Applied Physics, RAS, 603600, Nizhny Novgorod, Russia

It is shown that broadband optical continua may be generated as light propagates through a coherently prepared medium. Stimulated Raman scattering is a parametric process responsible for the spectral broadening. Even though the generation of spectral components is limited by the dispersion of the medium, numerical estimates for realistic parameters show feasibility of generating coherent optical continua with total bandwidth of several hundred terahertz without implementation of any dispersion compensating technique. Finally, a technique for producing broadband coherent optical spectra and, thus, ultrashort pulses of radiation is proposed.

PACS number(s): 42.50.Gy, 42.65.Dr, 42.65.Re

I. INTRODUCTION

During last two decades, progress in ultrashort pulse generation and amplification techniques resulted in the development of lasers generating extremely short (several femtoseconds) and very high-peak power (up to 10^{15} W) optical pulses [1]. Such an enormous result may be obtained by using different mode-locking techniques for ultrashort pulse generation combined with the idea of chirped pulse amplification. However, both generation and amplification of ultrashort pulses are usually based on the existence of active media with very broad (up to ~ 100 THz) amplification spectra, such as yttrium aluminum garnet YAG, sapphire, LiSAF, etc. doped with transition-metal ions. Thus, the duration of generated pulse and its wavelength are restricted by the parameters of these media.

In parallel with this progress, hollow-fiber and parametric amplification techniques resulted in generation of sub-10-fs pulses. These two techniques are considered the most advantageous since they allow for wide tunability of the generated pulses in combination with high-energy per pulse (see, for example, [2] and references therein).

A possibility of ultrashort pulse generation has been predicted theoretically [3] and confirmed experimentally [4] by Harris and Sokolov and Hakuta *et al.* It is based on a stimulated collinear Raman scattering of light as it propagates through the Raman medium. It has been shown that the efficiency of a Raman sideband generation can be very high if the excited Raman coherence is close to maximal. Therefore, very broad spectrum from near infrared (IR) up to vacuum ultraviolet (VUV) can be generated. It has been also shown that the generated spectrum allows pulse compression in a normally dispersive medium and that the pulse repetition rate is determined by the frequency of the Raman transition. However, as is well known, efficient coherence excitation at Raman transition is possible only if there is a population difference at this transition. This requires high frequency of this transition so that there is a population difference due to thermal distribution. In other works [3,4], the energy of Raman transition was chosen to be $(3-4) \times 10^3$ cm^{-1}. Such high frequency corresponds to the pulse repetition period 5–10 fs. Therefore, it is impossible to separate a single pulse from the sequence.

The only way to decrease the pulse repetition rate is to lower the frequency of the Raman transition. Thus, a mechanism of excitation of Raman coherence between equally populated levels must be proposed. In [5], it has been shown that low-frequency coherence may be excited due to relaxation processes at optical transitions that are typically neglected when considering Raman scattering. This effect originates from well-known coherent population trapping (CPT) (for review, see [6]). The technique proposed in [5] allows one to generate very broad coherent optical spectra (hundreds of teraherz) with rather low-frequency separation between the two subsequent sidebands (~ 1–10 GHz), which implies a low-pulse repetition rate after pulse compression. In fact, the idea presented in [5] is a generalization of the approach proposed by Sokolov and Harris. However, the efficiency of the CPT process is very low in the case of far-off-resonant electromagnetic field. Thus, the creation of Raman coherence requires rather intense fields and severe restrictions on the relaxation rates at both Raman and optical transitions. Besides that, very strong electromagnetic-field propagating in the medium may experience undesirable nonlinear self action, such as spatial self focusing, which might place a restriction on the length of propagation in the medium and, thus, significantly reduce the width of generated coherent spectrum.

In this paper, a possibility to avoid the difficulties, described in the previous paragraph, is proposed. It is connected to the idea that low-frequency Raman coherence may be prepared in the CPT process under the action of the external driving field resonant to the optical transition in the medium. Then, a rather weak probe field is scattered due to the excited coherence producing Raman sidebands with frequency separation equal to the frequency of the excited coherence. In this case, no self action of the probe field can occur. Moreover, the efficiency of Raman coherence preparation may be significantly increased due to the resonant character of interaction between the driving field and the medium. The situation is very similar to that described in the paper by Huss *et al.* [7]. In that work, a generation of four additional Raman sidebands in a coherently driven sodium vapor has been observed experimentally. The reason for the low efficiency of the sideband generation demonstrated in [7] is a very low density of active atoms ($\sim 10^{12}$–10^{13}
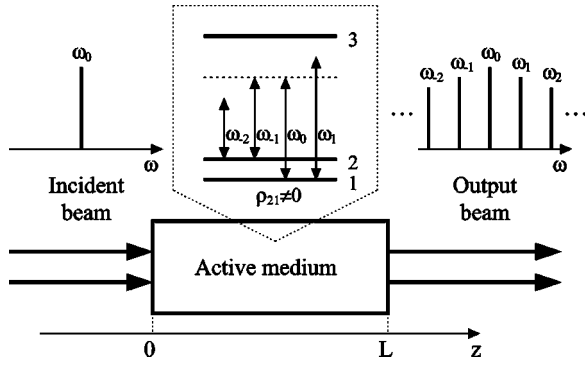
FIG. 1. The scheme of the interaction of a three-level medium with polychromatic electromagnetic field.

cm^{-3}). In this paper, it will be shown that at much higher densities it is possible to generate up to 10^4–10^5 additional Raman sidebands and, thus, produce very broad (~ 100 THz) coherent optical spectrum.

The outline of the paper is as follows. In Sec. II master equations describing the propagation of a polychromatic electromagnetic field through a coherently prepared medium will be derived. They describe the Raman sideband generation process. In Sec. III, the propagation equations for sidebands will be solved both analytically in the cases of no dispersion and linear group dispersion of the medium and numerically for the case of realistic dispersion. It will be shown that, even though the dispersion limits the generation of different Raman sidebands, it is still possible to generate coherent optical spectra with a total bandwidth of several hundred terahertz for real parameters of active medium. However, it requires a rather long propagation path and, thus, the necessity of exciting Raman coherence in very long (~ 1–2 m) samples. In Sec. IV, a cavity technique is proposed to reduce the length of the medium that should be driven. As it will be shown, exploiting cavity one may generate very broad optical continua without the need for driving long samples. Finally, in Sec. V, the process of coherent population trapping in the active medium will be considered in detail. It will be shown how the Raman coherence may be excited in an optically thick sample due to electromagnetically induced transparency (EIT) accompanying the CPT process. The combination of cavity technique (see, Sec. IV) and the possibility of CPT in an optically thick sample results in a very reliable and efficient technique for the generation of broadband coherent optical spectra that might compete with parametric amplification and hollow-fiber techniques. In the conclusion (Sec. VI) the main results of this paper will be summarized.

II. MODEL OF ATOMIC SYSTEM AND PROPAGATION EQUATIONS

Let us consider an interaction of a three-level Raman medium with an electromagnetic field consisting of equally spaced spectral components propagating along the z axis (see Fig. 1). The spectral components of the electromagnetic field are plain waves with no spatial structure in the transverse direction. A boundary problem of the Raman sideband gen-

eration, in which a monochromatic field of frequency ω_0 is incident onto the coherently prepared medium at $z=0$, is considered. The amplitude of the electric field in the electromagnetic probe wave inside the medium is given by

$$E = \frac{1}{2} \sum_k (E_k e^{-i\omega_k t} + \text{c.c.}), \tag{1}$$

where E_k is the local complex amplitude of each individual monochromatic wave, $\omega_k = \omega_0 + k\delta$ is its frequency, ω_0 is the carrier frequency of the wave packet, and δ is a frequency spacing between the two subsequent components. The amplitudes E_k are independent of time and $E_k(z=0) = 0$ for all k except $k=0$. The medium is assumed to be prepared by some external driving in a coherent state with the populations ρ_{11} and ρ_{22} for the ground-state sublevels and $\rho_{33}=0$ and the coherence $\rho_{21} = \sigma \exp(-i\delta t + i\kappa z)$, oscillating with frequency δ corresponding to the frequency difference of the two subsequent electromagnetic modes. Here, it is assumed that the complex amplitude of the coherence σ is neither time nor spatially dependent. It is also implied that the wave-number κ is independent of δ. The frequency of the transition $1 \leftrightarrow 2$ is chosen to be close to δ, so that the coherence at this transition may be efficiently excited by some external driving. The frequencies of the two optical transitions $3 \leftrightarrow 1,2$ are much larger than δ. The components of the electromagnetic field are tuned far from resonance with optical transitions, so that $|\omega_{31,32} - \omega_k| \gg \delta$ for all k. The dipole moments of the transitions $3 \leftrightarrow 1,2$ are chosen being equal: $\mu_{31} = \mu_{32} = \mu$. Finally, the incident electromagnetic field is assumed to be rather weak, so that it does not affect the populations ρ_{jj}, $j=1,2,3$, and the coherence ρ_{21}.

The equation for the amplitudes E_k may be written in the form

$$\frac{d^2 E_k}{dz^2} + \frac{\omega_k^2}{c^2} \varepsilon_k E_k = -\frac{8\pi}{c^2} \omega_k^2 P_k. \tag{2}$$

Here, ε_k is the dielectric constant of the medium for the frequency ω_k and P_k is the kth component of the polarization P associated with the Raman-active atoms

$$P = \sum_k (P_k e^{-i\omega_k t} + \text{c.c.}). \tag{3}$$

The polarization P is given by the following expression:

$$P = N Tr(\hat{\mu}\hat{\rho}) = N\mu(\rho_{13} + \rho_{31} + \rho_{23} + \rho_{32}), \tag{4}$$

where N is the density of active atoms and $\rho_{3j} = \rho_{j3}^*$ are the off-diagonal elements of the density matrix describing the atomic system. In turn, the evolution of ρ_{3j} is governed by the following set of equations:

$$\dot{\rho}_{3j} + i\omega_{3j}\rho_{3j} + i\frac{\mu E}{\hbar}(\rho_{33} - \rho_{jj} - \rho_{kj}) = -\Gamma\rho_{3j}, \tag{5}$$

where Γ is the relaxation rate of the optical coherences, $j,k = 1,2$, $j \neq k$. In further consideration, the detunings

$\omega_{31,32} - \omega_k$ are assumed to be much greater than the homogeneous optical linewidth Γ, thus, it is possible to neglect relaxation terms in the right-hand side of Eqs. (5). Moreover, the detunings $\omega_{31,32} - \omega_k$ are not assumed to be small compared to the carrier frequency and the frequencies of the optical transitions, i.e., the rotating-wave approximation is not valid. Thus, we seek the solution of the set of Eqs. (5) in the form

$$\rho_{3j} = \sum_k (u_{3j}^{(k)} e^{-i\omega_k t} + v_{3j}^{(k)} e^{i\omega_k t}). \tag{6}$$

The kth component of the optical polarization may be written as follows:

$$P_k = N\mu(u_{31}^{(k)} + v_{31}^{(k)*} + u_{32}^{(k)} + v_{32}^{(k)*}). \tag{7}$$

The steady-state solution for the amplitudes $u_{3j}^{(k)}$ and $v_{3j}^{(k)}$ is given by

$$u_{31}^{(k)} = \frac{\tilde{\Omega}_k \rho_{11} + \tilde{\Omega}_{k-1} \sigma e^{i\kappa z}}{\omega_{31} - \omega_k}, \tag{8}$$

$$u_{32}^{(k)} = \frac{\tilde{\Omega}_k \rho_{22} + \tilde{\Omega}_{k+1} \sigma^* e^{-i\kappa z}}{\omega_{32} - \omega_k}, \tag{9}$$

$$v_{31}^{(k)} = \frac{\tilde{\Omega}_k^* \rho_{11} + \tilde{\Omega}_{k+1}^* \sigma e^{i\kappa z}}{\omega_{31} + \omega_k}, \tag{10}$$

$$v_{32}^{(k)} = \frac{\tilde{\Omega}_k^* \rho_{22} + \tilde{\Omega}_{k-1}^* \sigma^* e^{-i\kappa z}}{\omega_{32} + \omega_k}, \tag{11}$$

where $\tilde{\Omega}_k = E_k \mu / 2\hbar$.

Seeking the solution of propagation Eq. (2) in the form $\tilde{\Omega}_k = \Omega_k e^{i\kappa_k z}$, where $\kappa_k = \omega_k \sqrt{\varepsilon_k}/c$, and assuming that the amplitudes Ω_k vary very slowly along the propagation path, it is easy to derive the propagation equation for amplitudes Ω_k

$$\frac{d\Omega_k}{dz} = i\tilde{\nu}_k (\Omega_k n_{12} + \Omega_{k-1} s_{12} e^{i(\kappa - \Delta\kappa_k)z}$$

$$+ \Omega_{k+1} s_{21} e^{i(\Delta\kappa_{k+1} - \kappa)z}). \tag{12}$$

Here, the following notations are introduced:

$$\tilde{\nu}_k = \frac{2\pi\omega_k \mu^2 N}{\hbar c^2 \kappa_k}, \quad \Delta\kappa_k = \kappa_k - \kappa_{k-1}, \tag{13}$$

$$n_{12} = 2\omega_k \left(\frac{\omega_{31}\rho_{11}}{\omega_{31}^2 - \omega_k^2} + \frac{\omega_{32}\rho_{22}}{\omega_{32}^2 - \omega_k^2} \right), \tag{14}$$

$$s_{12} = \sigma\omega_k \left(\frac{1}{\omega_{31} - \omega_k} + \frac{1}{\omega_{32} + \omega_k} \right), \tag{15}$$

$$s_{21} = \sigma^*\omega_k \left(\frac{1}{\omega_{31} + \omega_k} + \frac{1}{\omega_{32} - \omega_k} \right). \tag{16}$$

Equation (12) is the master equation describing the propagation of the electromagnetic field through the medium. In the next section, the solution of this equation will be found both analytically and numerically.

III. THE SOLUTION OF PROPAGATION EQUATION

In order to obtain the analytical solution of propagation Eq. (12), the following approximations are used. First, the constants n_{12}, s_{12}, and s_{21} are assumed to be independent of k. This is valid if the total width of the generated spectrum is much less than the one-photon detuning of the optical field from the resonance with optical transitions $1,2 \leftrightarrow 3$. Moreover, $s_{12} = s_{21}^* \equiv sn_{12}$ since $\delta \ll \omega_{31,32} \pm \omega_k$ for all k, thus, Eq. (12) may be rewritten in the following form:

$$\frac{d\Omega_k}{dz} = i\nu(\Omega_k + \Omega_{k-1} s e^{i(\kappa - \Delta\kappa_k)z} + \Omega_{k+1} s^* e^{i(\Delta\kappa_{k+1} - \kappa)z}), \tag{17}$$

where $\nu = \tilde{\nu} n_{12}$ and the quantities s and ν are evaluated at $\omega_k = \omega_0$.

In order to proceed with solving Eq. (17), one has to specify the refractive index $n_k = \sqrt{\varepsilon_k}$. In the simplest case of the refractive index being equal to n_0 independently of k (no dispersion), one has $\Delta\kappa_k = \delta n_0/c \equiv \Delta\kappa$. Introducing Fourier transformation as

$$B(u,z) = \sum_k \Omega_k e^{iuk}, \tag{18}$$

one may obtain the equation for amplitude B:

$$\frac{dB}{dz} = iB\nu(1 + se^{i[u + (\kappa - \Delta\kappa)z]} + s^* e^{-i[u + (\kappa - \Delta\kappa)z]}). \tag{19}$$

Taking into account the boundary condition at $z = 0$, one obtains its solution:

$$B(u,z) = \Omega_0 e^{i\nu z} \exp\left[\frac{4i\nu|s|}{\Delta\kappa'} \sin\frac{\Delta\kappa' z}{2} \cos\left(\frac{\Delta\kappa' z}{2} + u + \varphi \right) \right], \tag{20}$$

where $\Delta\kappa' = \kappa - \Delta\kappa$ and φ is the phase of coherence s defined as $s = |s|e^{i\varphi}$. One may easily find the solution for Ω_k in terms of Bessel functions

$$\Omega_k = \frac{1}{2\pi} \int_0^{2\pi} B e^{-iuk} du = i^k \Omega_0 e^{i\nu z} J_k\left(\frac{4\nu|s|}{\kappa - \Delta\kappa} \sin\frac{(\kappa - \Delta\kappa)z}{2} \right). \tag{21}$$

It is clearly seen that the amplitude of Ω_k is a periodic function of z if $\kappa \neq \Delta\kappa$. Thus, the efficient Raman sideband generation is limited by the distance $L = \pi/(\kappa - \Delta\kappa)$ when the relative phase of the two subsequent sidebands equals to π. However, if $\kappa = \Delta\kappa = \delta n_0/c$, the sideband generation process is efficient at any length, and, therefore, one may generate a arbitrarily wide spectrum. The number of generated sidebands is proportional to the length of the medium, the

amplitude of the coherence $|s|$, and the propagation constant ν. The total generated bandwidth may be estimated as $\Delta\omega = 4\nu|s|L\delta$, where L is the length of the active medium.

Let us now consider a more realistic case in which the refractive index n_k depends on k linearly

$$n_k = n_0 + \left.\frac{\partial n}{\partial\omega}\right|_{\omega=\omega_0} k\delta = n_0 + n_1 k\delta. \qquad (22)$$

In this case, the propagation equation reads as follows:

$$\frac{d\Omega_k}{dz} = i\nu[\Omega_k + (s\Omega_{k-1}e^{i(\phi_1 - 2\kappa_1 k)z}$$

$$+ s^*\Omega_{k+1}e^{-i(\phi_1 - 2\kappa_1 k)z})e^{i\kappa_1 z}], \qquad (23)$$

where $\phi_1 = \kappa - (n_0 + n_1\omega_0)\delta/c$ and $\kappa_1 = n_1\delta^2/c$. Thus, the condition for κ should be modified in order to make the sideband generation process more efficient, so that $\phi_1 = 0$. However, even under this condition, phase mismatch is not eliminated completely. The sideband generation process stops when the relative phase of the two subsequent sidebands $2\kappa_1 kz$ becomes equal π. Using this fact, one may easily estimate the total width of the spectrum that can be generated. The number of generated sidebands is $k_{gen} = 4\nu|s|z$, therefore, the length of the medium must satisfy the following condition:

$$2\kappa_1 L\frac{k_{gen}}{2} = 4n_1|s|\nu\delta^2 L^2/c < \pi. \qquad (24)$$

The total width of the generated spectrum is then given by the following expression:

$$\Delta\omega_{tot} \sim 2\sqrt{\frac{\pi c|s|\nu}{n_1}}. \qquad (25)$$

Let us now turn to the estimates for real media. In order to generate wider spectrum, one should have a high density of active atoms. Such densities may be achieved in solid-state media. On the other hand, the coherence decay rate at the transition $1\leftrightarrow 2$ should be low, so that one could excite maximal coherence $|s|$. This condition is typically satisfied at Zeeman transitions in rare-earth doped solid hosts at low temperatures. Moreover, as it has already been shown, the repetition rate of a generated pulse sequence is determined by the frequency of Raman transition. Thus, in order to obtain a rather low repetition rate (several gigahertz) one has to use Zeeman or hyperfine transitions, whose frequencies lie in the desired range. The third condition is the existence of a rather broad spectral region in which the absorption of light is low. Typically, rare earths in solid hosts have many $4f^n$ levels inside the band gap, so that it is rather hard to find a broad spectral region that does not contain any $4f^n\leftrightarrow 4f^n$ transitions that may cause the absorption of generated sidebands. However, there is at least one exception, namely, cerium in different solid hosts. This rare-earth metal typically enters solids in a trivalent state. Ce^{3+} ion has only one electron in a $4f$ shell. The structure of electronic levels of Ce^{3+}
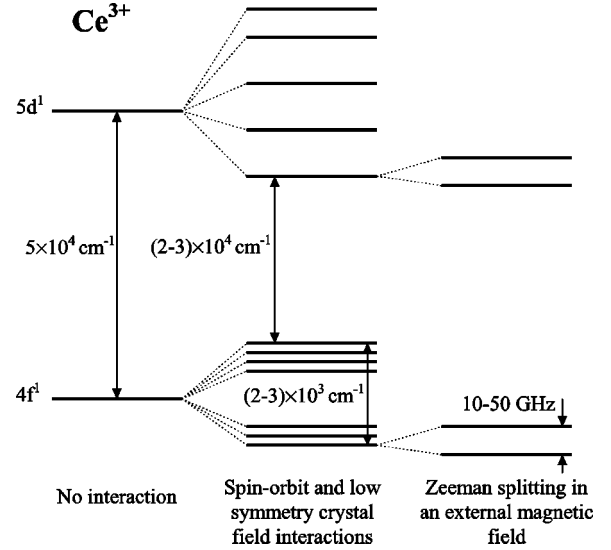
FIG. 2. Energy level scheme of Ce^{3+} ion in a site of low symmetry.

in a low-symmetry site is shown in Fig. 2. One can see that there is a wide region of transparency for this ion from near IR ($3-4$ μm) up to UV (~ 300 nm). Furthermore, $4f^1\leftrightarrow 5d^1$ transitions of Ce^{3+} are electric-dipole allowed, which makes the efficiency of stimulated Raman scattering rather high.

For the estimates, the following parameters will be used. The wavelength of the lowest $4f^1\leftrightarrow 5d^1$ transition is chosen 350 nm, which is a typical value for most crystals containing cerium [8]. One of the exceptions is Ce^{3+}:YAG for which this wavelength is close to 500 nm. The population decay rate of the $5d^1$ state varies in the range $40-60$ ns, thus, it is natural to take it being equal to 50 ns. This allows one to calculate the dipole moment of the optical transitions. The carrier wavelength is chosen $\lambda_0 = 500$ nm. The case of maximal coherence $|s| = 1/2$ is considered, which implies that $\rho_{11} = \rho_{22} = 1/2$. The refractive index of the medium is approximated by the one-oscillator formula:

$$n^2 = 1 + \frac{A\lambda^2}{\lambda^2 - B^2}, \qquad (26)$$

where A and B are constants. This relation will be used to calculate n_0 and n_1 for the estimates. Moreover, it will be exploited in order to calculate κ_k for each sideband in the numerical simulations. Typically, for real crystals, A lies within the range $1.5-2.5$ (for YAG $A = 2.28$ [9]) and $B \sim 100$ nm ($B = 109$ nm for YAG). For the estimates $A = 2$ and $B = 100$ nm are chosen. All these data allow one to derive the propagation constant $\nu = 85$ cm^{-1}. The linear dispersion is described by $n_1 = 1.3\times 10^{-17}$ s. Thus, it is possible to estimate the maximal width of generated spectrum $\Delta\omega_{tot} \approx 2\pi\times 180$ THz. This value corresponds to the pulse duration ~ 10 fs. It is worth noting that this value may be achieved without any dispersion compensating technique. Now, it is possible to estimate the length at which this spectrum is generated. For $\delta = 2\pi\times 10$ GHz, which corresponds
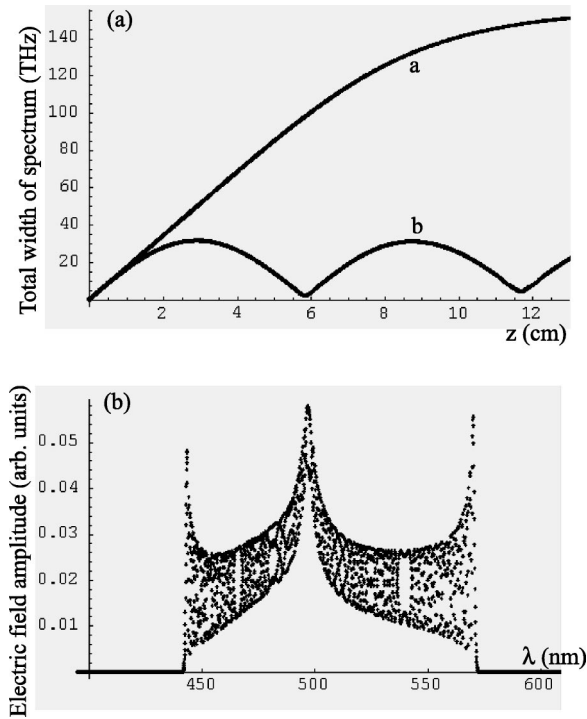
FIG. 3. (a) The dependence of the total generated bandwidth on the propagation distance is shown. Curves a and b indicate spectral bandwidths with and without correction for linear dispersion, respectively. (b) Raman sideband electric-field amplitudes are plotted against the wavelength at $z \approx 13$ cm. Amplitudes are normalized with respect to the amplitude of the incident field. Approximately, 1500 sidebands are generated.

to the pulse repetition period 0.1 ns, 1.8×10^4 sidebands may be generated. This requires a propagation length $L \sim 100$ cm.

Now, it is needed to present the results of numerical simulation of Eq. (12). They are shown in Fig. 3. Unlike the previous discussion, no approximations have been used in this simulation except that the absorption of the optical field has been neglected. This means that Eqs. (13)–(16) are used to calculate coefficients in Eq. (12) and Eq. (26) is used to calculate κ_k for each sideband. All the parameters used in it were taken the same as in the previous paragraph except δ, which is now chosen to be $2\pi \times 100$ GHz. This choice of δ has been made in order to make numerical calculations not very time consuming. However, the presented results confirm analytical estimates for the width of the generated spectrum and the required length of the medium. The wave number of the coherence κ is chosen to be equal to $(n_0 + n_1\omega_0)\delta/c$ where n_1 is calculated at frequency ω_0. Figure 3(a) shows the dependence of the total width of the generated spectrum on the propagation length. For comparison, the width of the generated spectrum, when the correction for linear dispersion $n_1\omega_0\delta/c$ is neglected, is plotted as well. In Fig. 3(b), the amplitudes of generated sidebands are plotted against the sideband number at $L = 13$ cm. It can be seen that the sidebands with higher frequencies are generated more efficiently since they are closer to the resonance with an optical transition. According to the analytical estimates, the efficient gen-
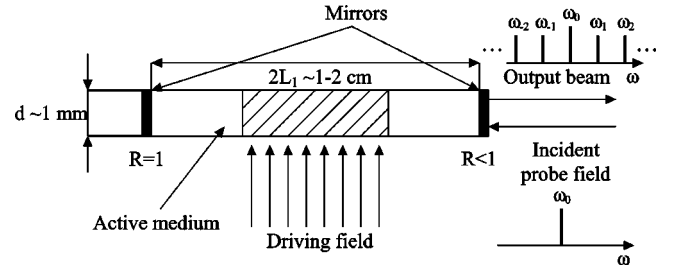
FIG. 4. Cavity technique of broadband optical continua generation. The length of the driven part of the medium is $L_1 \sim 1$ cm for $\delta \sim 10$ GHz and for the other parameters specified in the text.

eration of new sidebands should stop at $L \approx 10$ cm. This value is qualitatively consistent with $L \approx 13$ cm obtained in the numerical simulation. Finally, the total bandwidth 150 THz well coincides with analytical estimate 180 THz. Thus, for $\delta = 2\pi \times 10$ GHz, the same bandwidth of generated signal can be obtained but for $L = 130$ cm.

As is clearly seen, a rather long propagation length is required in order to generate coherent optical continua with the total bandwidth ~ 100 THz. For such a long propagation path, absorption of the probe field should be taken into account. In order to compare the propagation length required to obtain the maximal width of generated spectrum with absorption length, let us take YAG doped with cerium as an example of an active medium. For pure YAG, it is known that the absorption coefficient in near IR and red is 1.5×10^{-3} cm^{-1}, while for green and yellow light it is $3-4 \times 10^{-3}$ cm^{-1}. These values correspond to the absorption length $2.5-6$ m which is larger than the required 130 cm. Another contribution to the absorption of the probe light comes from dopant ions Ce^{3+}. The main contribution to the absorption associated with cerium originates from the lowest $4f^1$-$5d^1$ transition. The estimates for this absorption channel give absorption length $2-3$ m for concentration 10^{20} cm^{-3} of cerium ions in the case of a rather large ($\sim 10^4$ cm^{-1}) detuning of the probe field from the resonance with the $4f^1$-$5d^1$ transition. Thus, the generation length appears to be less than the absorption one. This means that optical continuum may be generated almost without loss of energy.

So far, the coherence σ_{21} was assumed given. However, it is difficult to excite low-frequency coherence in such a long sample. In the next section, it will be shown how this difficulty can be avoided by using cavity technique.

IV. EXPLOITING CAVITY TO REDUCE THE LENGTH OF THE MEDIUM

Let us discuss how the experimental setup should be arranged in order to generate coherent broadband optical spectra according to the technique proposed in Sec. III. As it was mentioned, the propagation length of the probe field inside the crystal should be fairly large (several tens of centimeters). It is very difficult to produce a low-frequency coherence in such a long sample. In order to avoid this difficulty, one may use cavity as it is shown in Fig. 4. The driving field illuminates the active medium in the direction perpendicular to the direction of the propagation of the probe field. How-
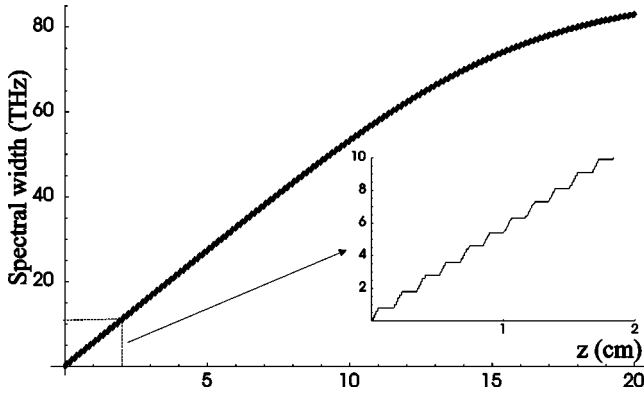
FIG. 5. The dependence of the total spectral bandwidth on the propagation distance inside the cavity. Spectral broadening at each pass through the active medium can be seen. The maximal bandwidth correspond to ≈ 120 passes through the medium.

FIG. 6. Coherent population trapping in a three-level medium.

ever, as it is already known from Eq. (21), the phase matching condition for the probe field is not satisfied in this case.

In order to fulfill the phase-matching condition, one has to introduce spatial modulation of the coherence σ_{21} with wave-number $\kappa = (n_0 + n_1\omega_0)\delta/c$. This may be done by illuminating only the central half of length $L_1 = \pi c/\delta(n_0 + n_1\omega_0)$ of the sample. In this case, the propagation process may be described in the following way: First, the probe field propagates through the illuminated medium and generates Raman sidebands. When the generation process stops, the probe field starts propagating through the part of the sample without coherence. During this stage, Raman sidebands gain additional phase, so that when they come back to the illuminated part of the sample, they have right phases to continue the generation of sidebands. The lengths of the two parts of the medium that are not illuminated by the driving field should be exactly $L_1/2$, thus, the total length of the medium inside the cavity is $2L_1$. The estimates for the same parameters as were used in Sec. III and for $\delta = 2\pi \times 10$ GHz give $L_1 \approx 8.29$ mm.

At each pass through the driven part of the medium, about 100 sidebands are generated. Thus, in order to generate broadband spectrum, the probe field should pass through the medium several tens or even several hundred times. The reflection coefficient of the output mirror should be adjusted so that the number of passes of the probe beam through the cavity corresponds to the maximal width of the generated spectrum. The width of the spectrum plotted vs the propagation length is shown in Fig. 5. In this simulation, the frequency of Raman transition is chosen $\delta = 2\pi \times 100$ GHz for the same reason as in Sec. III, while the other parameters are the same as for the previous simulation. In this case, $L_1 = 0.83$ mm. One can see the change in the spectral bandwidth at each pass through the active part of the medium. It should be noted that in this case, the generation process is approximately two times less efficient compared to the case considered in Sec. III. This is due to the fact that now only half of the medium participates in the generation process while the dispersion is determined by the whole sample. However, this technique allows for efficient driving of the
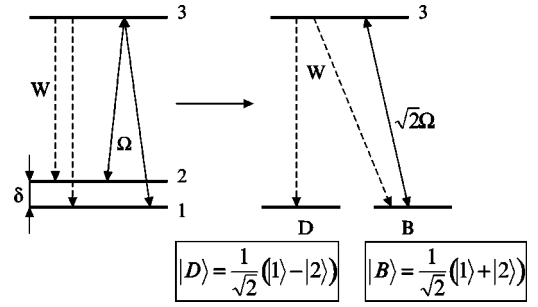
medium even though the efficiency of spectral broadening is slightly reduced.

The transverse dimensions of the sample are limited by the divergence due to diffraction. It is easy to find that for the propagation path ~ 1 m and the wavelength 500 nm the transverse size of the probe beam should be ~ 1 mm. This value is much greater than the absorption length of the driving field (~ 10–20 μm). However, as it has been pointed out in the introduction, the propagation length of the driving field may be increased significantly due to EIT accompanying the CPT process. This will be discussed in the next section.

In fact, the limitation placed on the transverse dimensions of the sample by diffraction may be removed by using spherical mirrors for the cavity. However, fabrication of such tiny mirrors with appropriate curvature and a certain reflection coefficient in a huge-frequency range seems to be troublesome.

V. CREATION OF LOW-FREQUENCY COHERENCE

Let us discuss how low-frequency coherence at Raman transition may be established by means of CPT. As is well known, CPT is a process in which each atom is prepared in a coherent superposition of the two ground-state sublevels (so-called "dark" state) via spontaneous decay from the upper level. This situation is illustrated in Fig. 6. In order to prepare an ensemble of atoms in a "dark" state, each atom should absorb at least one photon from the driving field and consequently decay. Thus, the energy required to prepare n_{at} atoms in the "dark" state is at least $E_{dark} = n_{at}\hbar\omega$, where ω is the frequency of the driven optical transition (here, it is assumed that ω_{31} and ω_{32} are very close to each other: $\omega_{31} = \omega_{32} = \omega$). For the above example of crystal doped with Ce^{3+} and the dimensions of the illuminated part as shown in Fig. 4, one obtains $n_{at} \sim 10^{18}$ and $E_{dark} \sim 0.5$–1 J. Furthermore, the coherence at Raman transition $1 \leftrightarrow 2$ should be created (i.e., the "dark" state should be populated) much faster than it decays. Typically, for Zeeman transitions in rare-earth ions, the transverse relaxation-time T_2, determined primarily by spin-lattice relaxation, may be as low as 10^2 s^{-1} at low temperatures [10]. Thus, one comes to the parameters of the driving pulse. It should have total energy E_{dark} and duration τ: $T_2 \gg \tau \gg W^{-1}$.

In order to give quantitative description of CPT in an optically thick medium, let us consider the following model:
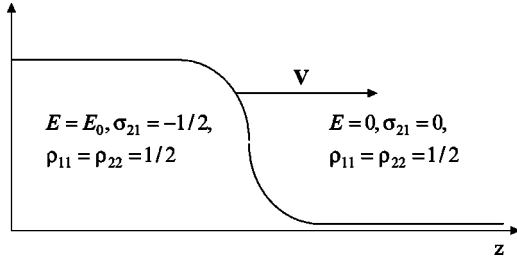
FIG. 7. The structure of the kink-type wave of coherence propagating inside optically thick medium.

The medium is assumed to be infinite along the propagation direction of the driving field (see Fig. 7). There is no coherence σ_{21} at $z=+\infty$, the populations of the two ground-state sublevels are half, and there is no driving field in this region. A bichromatic electromagnetic field, whose frequency components are resonant to the transitions $3\leftrightarrow1$ and $3\leftrightarrow2$, is incident on the medium at $z=-\infty$. The intensities of the field components are assumed being equal: $E_1=E_2=E$. The corresponding Rabi frequency $\Omega=E\mu/2\hbar$ where it is implied that $\mu_{31}=\mu_{32}=\mu$. In this region, the coherence at Raman transition is maximal and equal to $-1/2$ which implies that σ_{21} does not decay. It is clear that there is some intermediate region in which the medium becomes coherently prepared. Moreover, this region should move in the positive direction of the z axis since the CPT process makes the medium transparent and allows the driving field to penetrate further. It is easy to derive the set of equations that describes both the medium and the electromagnetic field. After elimination of optical coherences, one obtains

$$\frac{\partial\rho}{\partial t}-\frac{2\Omega^2}{\Gamma}(1-3\rho-\sigma_{21})=W(1-2\rho), \tag{27}$$

$$\frac{\partial\sigma_{21}}{\partial t}-\frac{2\Omega^2}{\Gamma}(1-3\rho-\sigma_{21})=0, \tag{28}$$

$$\frac{\partial\Omega}{\partial z}+\frac{\kappa_d}{\omega}\frac{\partial\Omega}{\partial t}=\frac{2\pi N\mu^2\omega^2}{c^2\hbar\Gamma\kappa_d}\Omega(1-3\rho-\sigma_{21}). \tag{29}$$

Here, $\rho_{11}=\rho_{22}=\rho$, Γ is the optical linewidth, and κ_d is the driving field wave number. The two driving fields are assumed to be in exact resonance with transitions $3\leftrightarrow1$ and $3\leftrightarrow2$. This set of equations has two steady-state spatially uniform solutions, one is $\Omega=0$, $\sigma_{21}=0$, $\rho=1/2$, and the other one is $\Omega=\Omega_0$, $\sigma_{21}=-1/2$, $\rho=1/2$, with Ω_0 being arbitrary constant.

As was mentioned above, there should exist a solution moving in the positive z direction. Let us seek this solution in the form $\rho=\rho(t-z/v)$, $\sigma_{21}=\sigma(t-z/v)$, and $\Omega=\Omega(t-z/v)$, where v is the velocity of propagation of this solution. Thus, the Eqs. (27)–(29) will take the following form:

$$\rho'-\frac{2\Omega^2}{\Gamma}(1-3\rho-\sigma)=W(1-2\rho), \tag{30}$$

$$\sigma'-\frac{2\Omega^2}{\Gamma}(1-3\rho-\sigma)=0, \tag{31}$$

$$\Omega'\left(\frac{\kappa_d}{\omega}-\frac{1}{v}\right)=\frac{2\pi N\mu^2\omega^2}{c^2\hbar\Gamma\kappa_d}\Omega(1-3\rho-\sigma). \tag{32}$$

Here, prime represents the derivative of the corresponding function with respect to its argument. It can be seen from the last two equations that there exists one integral

$$\Omega^2\left(\frac{\kappa_d}{\omega}-\frac{1}{v}\right)-\frac{2\pi N\mu^2\omega^2}{c^2\hbar\kappa_d}\sigma=\text{const.} \tag{33}$$

Taking into account the boundary condition at $t-z/v=-\infty$ ($\Omega=0$, $\sigma=0$), one finds that const$=0$. Using the boundary condition at $t-z/v=+\infty$ ($\Omega=\Omega_0$, $\sigma=-1/2$), it is easy to find the velocity of the front propagation

$$v=1/\left(\frac{\kappa_d}{\omega}+\frac{\pi N\mu^2\omega^2}{c^2\hbar\kappa_d\Omega_0^2}\right)=1/\left(\frac{\kappa_d}{\omega}+\frac{\hbar\omega N}{I_0}\right). \tag{34}$$

Here, I_0 is the intensity of the driving field at $t-z/v=+\infty$. The last term in the denominator of this expression is much greater than the first one at high densities ($N\sim10^{20}$ cm^{-3}) and any achievable intensities of the driving field. Thus, one obtains

$$v=\frac{I_0}{N\hbar\omega} \tag{35}$$

for the velocity of the front. So, if one wants to create low-frequency coherence in a sample of thickness L during time τ, the intensity of the driving field should be

$$I_0=\frac{LN\hbar\omega}{\tau}. \tag{36}$$

The corresponding energy per unit area in the driving pulse is $I_0\tau=LN\hbar\omega$. This value exactly matches the qualitative estimates given in the first paragraph of this section.

It is also interesting to investigate the structure of this solution. If the intensity of the driving field is lower than the saturating intensity ($\Omega_0^2\ll\Gamma W$), the populations of the ground-state sublevels are always half. Taking into account the relation between σ and Ω (33), one comes to the following equation for the coherence σ:

$$\sigma'-\frac{2\sigma\Omega_0^2}{\Gamma}(1+2\sigma)=0. \tag{37}$$

Its solution has the following form:

$$\sigma=-\frac{1}{2+\exp\left[-\dfrac{2\Omega_0^2}{\Gamma}(\xi-\xi_0)\right]}, \tag{38}$$

where $\xi=t-z/v$ and ξ_0 is a constant that determines the initial position of the moving solution. The characteristic

length $L_c = v\Gamma/\Omega_0^2$, which determines the spatial structure of the obtained kink solution, well coincides with the absorption length of the driving field in the medium.

Thus, the conclusion is the following: In order to prepare the sample in a coherent ''dark'' state, a pulse of bichromatic resonant radiation with total energy $E_{dark} = n_{at}\hbar\omega$ and duration τ, $T_2 \gg \tau \gg W^{-1}$, is required. The estimates given in the beginning of the section show that the required parameters are reasonable, thus, making the establishing of low-frequency coherence feasible.

VI. CONCLUSION

A possibility of an efficient generation of broadband optical continua, based on stimulated Raman scattering of the light propagating through a coherently driven medium, is predicted. The proposed technique allows one to generate very broad (~ 100 THz) optical continua in almost any desired frequency range. The most striking feature of the proposed way of generating coherent optical continua is that no dispersion compensation technique is required. Moreover, the implementation of phase-correction techniques, such as chirped mirrors and diffraction grating pairs, may increase generated spectral bandwidth by several times, thus, making it possible to produce even subfemtosecond pulses of optical radiation.

[1] T. Brabec and F. Krausz, Rev. Mod. Phys. **72**, 545 (2000).

[2] G. Gerullo, S. De Silvestri, and M. Nisoli, *et al.*, IEEE J. Sel. Top. Quantum Electron. **6**, 948 (2000); R. L. Fork, G. H. Brito Cruz, P. C. Becker, and C. V. Shank, Opt. Lett. **12**, 483 (1987); M. Nisoli, S. De Silvestri, O. Svelto *et al.*, *ibid.* **22**, 522 (1997); A. Baltuska, Z. Wei, M. S. Pshenichnikov, and D. A. Wiersma, *ibid.* **22**, 102 (1997).

[3] S. E. Harris and A. V. Sokolov, Phys. Rev. Lett. **81**, 2894 (1998); S. E. Harris and A. V. Sokolov, Phys. Rev. A **55**, R4019 (1997); F. L. Kien, J. Q. Liang, and M. Katsuragawa *et al.*, *ibid.* **60**, 1562 (1999).

[4] A. V. Sokolov, D. R. Walker, D. D. Yavuz, G. Y. Yin, and S. E. Harris, Phys. Rev. Lett. **85**, 562 (2000); K. Hakuta, M. Suzuki, M. Katsuragawa, and J. Z. Li, *ibid.* **79**, 209 (1997).

[5] R. Kolesov and O. Kocharovskaya, Phys. Rev. Lett. (to be published).

[6] E. Arimondo, *Coherent Population Trapping in Laser Spectroscopy,* edited by E. Wolf, Progress in Optics Vol. XXXV (North-Holland, Amsterdam, 1996), p. 259

[7] A. F. Huss, N. Peer, R. Lammegger, E. A. Korsunsky, and L. Windholz, Phys. Rev. A **63**, 013802 (2001).

[8] P. Dorenbos, J. Lumin. **91**, 155 (2000).

[9] D. E. Zelmon, D. L. Small, and R. Page, Appl. Opt. **37**, 4933 (1998).

[10] I. N. Kurkin and K. P. Chernov, Zh. Exp. Teor. Fiz. **83**, 1072 (1982); M. H. North and H. J. Stapleton, J. Chem. Phys. **66**, 4133 (1977).